Supporting Information

Beaty et al. 10.1073/pnas.1713532115

SI Results

Background Connectivity Analyses. Previous research has indicated that coactivations of brain regions can increase correlations (i.e., functional connectivity) by introducing a common timing structure (1). We thus sought to verify that our model does not rely on task-evoked coactivation patterns to predict individual differences in creativity by performing analyses on background connectivity. Specifically, we modeled the effect of task using the CONN toolbox and calculated functional connectivity matrices using the residuals of this regression. All other preprocessing steps were identical to those described in the main text.

Performing leave-one-subject-out cross-validation in our initial training data set with these new connectivity matrices, we found similar predictive power for the high-creativity network [$r(161) = 0.32$, $P = 2.76e{-}05$] but not the low-creativity network [$r(161) = 0.15$, $P = 0.05$], which in the main text we describe as less reliable. The networks themselves showed considerable overlap with those visualized in Fig. 1. External validation revealed that the high-creativity network model generalized to predict creativity from functional connectivity in both the first external task validation sample [$n = 39$; $r(37) = 0.47$, $P = 0.002$], as well as the second [$n = 54$; $r(52) = 0.32$, $P = 0.02$], and generalized to predict creativity in a third independent group from resting-state functional connectivity [$n = 405$; $r(403) = 0.10$, $P = 0.04$]. Numeric differences in the results do not affect our main conclusion that models based on patterns of functional connectivity predict individual differences in creativity in novel individuals and datasets.

Partial Correlation Analyses. The Pearson correlations reported in the main text reflect associations between creative thinking ability and network connectivity strength. However, because creativity scores were moderately correlated with in-scanner motion in the original dataset, we sought to determine whether brain-behavior relations reported in the text were robust to subject motion. Here, we hence report partial correlations between observed and predicted creativity scores in the original dataset, and correlations between creativity scores and network strength in the external validation datasets—controlling for mean in-scanner motion values. Regarding the original dataset, we found that controlling for motion resulted in slightly attenuated correlations between observed and predicted creativity scores in the high-creative [$r(160) = 0.28$, $P < 0.001$] and low-creative [$r(160) = 0.19$, $P = 0.01$] networks. In the first task validation dataset ($n = 39$), we found a slight increase in the correlation between creativity scores and network strength in the high-creative network [$r(36) = 0.42$, $P = 0.009$] and a similarly small and nonsignificant correlation between creativity scores and low-creative network strength [$r(36) = -0.08$, $P = 0.65$]. Regarding the second task validation dataset ($n = 54$), we found a comparable pattern of correlations as previously reported for both the high-creative network [$r(51) = 0.29$, $P = 0.04$] and low-creative network [$r(51) = -0.02$, $P = 0.91$]. Likewise, regarding the resting-state dataset ($n = 405$), the previously reported effects were largely similar for both the high-creative network [$r(402) = 0.13$, $P = 0.01$] and low-creative network [$r(402) = 0.10$, $P = 0.04$].

SI Materials and Methods

External Validation 1: Task fMRI.

Participants. Behavioral and functional imaging data were reanalyzed from a previous study that assessed brain activity during the AUT (2). The total sample included 39 participants (26 female, mean age = 22.50 y, SD = 3.12). All participants were right-handed with normal or corrected-to-normal vision and reported no history of neurological disorder, cognitive disability, or medication that affects the central nervous system. Participants completed consent forms and were paid for their time. The study was approved by the local ethics committee of the University of Graz.

fMRI task paradigm. Participants completed the AUT during functional imaging. Similar to the above design and previous studies, the task involved generating unusual and creative uses for everyday objects. A unique feature of this paradigm, however, was that it allowed continuous idea generation over extended trial durations (i.e., 1 min vs. 12 s in study 1): Participants spontaneously generated ideas in a self-paced fashion and vocalized them as soon as they came to mind. Functional imaging data were acquired in a single run that included 15 task blocks. A trial block consisted of a jittered fixation cross (20–22 s) followed by a thinking period presetting an object cue (60 s) where participants were required to think of creative uses. Participants continuously generated ideas during the thinking period and vocalized their responses into a mouthpiece fixed to the head coil; the mouthpiece led to a microphone located outside the scanning room where an experimenter transcribed the responses. After the scan, participants were presented with their responses and asked to label each as "old" (i.e., recalled from memory) or "new" (i.e., generated on the spot). In lieu of a control task, the study contrasted neural activity associated with the generation of old vs. new ideas. However, for the current analysis, we analyzed data from the entire functional run, consistent with the seminal studies using cpm (3).

Behavioral assessment. Participants' verbal responses to the AUT were scored for creative quality by three trained raters using a subjective scoring method; raters used a four-point scale to code responses (1 = uncreative, 4 = very creative) and were instructed to consider both the originality and appropriateness of each idea into a single rating. Analysis of rater agreement showed good interrater reliability (ICC = 0.78). A fluency score was also computed for each participant by summing the total number of ideas generated for each trial and computing an average across the 12 trials. In addition to the in-scanner task responses, participants also completed laboratory-based AUT measures. Participants were given 2 min to type unusual and creative uses for everyday objects. Responses were similarly scored for fluency and originality by trained raters. A composite AUT score was computed for each participant by averaging the in-scanner and laboratory-based originality and fluency ratings.

MRI data acquisition and preprocessing. Participants completed the tasks in a single fMRI run. Whole-brain imaging was performed on a 3T Tim Trio system (Siemens Medical Systems) using a 32-channel head coil. BOLD-sensitive T2*-weighted functional images were acquired using a single shot gradient-echo EPI pulse sequence (TR = 2,000 ms, TE = 25 ms, flip angle = 90°, 34 axial slices, slice thickness = 3 mm, FoV = 192 × 192 mm, interleaved slice ordering) and corrected online for head motion. The first two volumes were discarded to allow for T1 equilibration effects. A high resolution T1 scan was acquired for anatomic normalization. Visual stimuli were presented using Presentation software (Neurobehavioral Systems) and viewed through a mirror attached to the head coil. Functional volumes were slice time-corrected and realigned using SPM 12, anatomically coregistered, normalized to the MNI template brain (Montreal Neurological Institute), and smoothed with a 6-mm^3 isotropic Gaussian kernel. [Note that smoothing kernels varied across datasets because, in some cases, only preprocessed data (i.e., smoothed images) were available for reanalysis.]

Task-related functional connectivity was assessed using the CONN toolbox (4) in MATLAB using the same preprocessing procedures described above, including regression of verbal response onsets and durations. For functional network construction, the mean BOLD signal was extracted from each ROI during the thinking period of the AUT (12 trials, 60 s; collapsing across trials). [Whole-brain correlation matrices were computed for all external validation analyses presented here, but only those nodes and edges in the high- and low-creative networks (i.e., those retained after statistical thresholding) were considered when computing network strength values in the validation samples.]

External Validation 2: Task fMRI.

Participants. Behavioral and functional imaging data were reanalyzed from a previous study that assessed brain activity during the AUT (5). The sample included 54 participants (26 female, mean age = 24.06 y, SD = 2.99). All participants were right-handed with normal or corrected-to-normal vision and reported no history of neurological disorder, cognitive disability, or medication that affects the central nervous system. Participants completed consent forms and were paid for their time. The study was approved by the local ethics committee of the Medical University of Graz.

fMRI task paradigm. Participants completed a creative thinking and control task during functional imaging: an AUT and an instances task (IT). In the AUT, participants were presented with a common object and required to generate unusual and original uses for it; in the IT—the control task—participants were presented with an adjective and required to generate conditions or facts related to it (6); the AUT and IT trials were presented in a random order. In the current analysis, we were primarily interested in extracting neural activity during the AUT, but we also assessed activity during the IT to test the sensitivity of the prediction model to the cognitive process engaged. Participants continuously generated responses to the AUT or the IT during an idea generation period. Functional imaging data were acquired in a single run that included 40 trials of each condition. A trial consisted of a jittered fixation cross (4–8 s), a thinking period presenting a cue word (a noun in the AUT or an adjective in the IT; 15 s), and a verbal response period requiring participants to speak their responses into an MRI-compatible microphone (7 s); an experimenter recorded verbal responses online for subsequent analysis of idea quality.

Behavioral assessment. Participants' verbal responses to the AUT were scored for originality by four trained raters using a subjective scoring method; raters used a four-point scale to code responses (0 = not at all original, 3 = very original) and were instructed to consider both the originality and appropriateness of each idea into a single rating. Analysis of rater agreement showed good interrater reliability (ICC = 0.75). A fluency score was also computed for each participant by summing the total number of ideas generated for each trial and computing an average across the 12 trials. A composite AUT score was computed for each participant by averaging the originality and fluency ratings.

MRI data acquisition and preprocessing. Participants completed the tasks in a single fMRI run. Whole-brain imaging was performed on a 3T Siemens Magnetom Skyra (Siemens Medical Systems) using a 32-channel head coil. BOLD-sensitive T2*-weighted functional images were acquired using a single shot gradient-echo EPI pulse sequence (TR = 2,400 ms, TE = 30 ms, flip angle = 90°, 36 axial slices, slice thickness = 3.5 mm, FoV = 240 mm) and corrected online for head motion. The first two volumes were discarded to allow for T1 equilibration effects. A high resolution T1 scan was acquired for anatomic normalization. Visual stimuli were presented using Presentation software (Neurobehavioral Systems) and viewed through a mirror attached to the head coil. Functional volumes were slice time-corrected and realigned using SPM 8, normalized to the MNI template brain (Montreal Neurological Institute), and smoothed with an 8-mm^3 isotropic Gaussian kernel; verbal response onsets and durations were also regressed from the BOLD signal. Functional connectivity was similarly assessed using the CONN toolbox (4) in MATLAB. As described above, the Shen anatomical atlas was used to define whole-brain networks. Here, we extracted mean BOLD signal from the 268 ROIs during the AUT and IT separately (20 trials each, 15 s; collapsing across trials); bivariate correlations were computed between each pair of ROIs, resulting in a 268 × 268 correlation matrix for each of the 54 participants.

External Validation 3: Resting-State fMRI.

Participants. Resting-state functional imaging data were obtained from the Southwest University Longitudinal Imaging Multimodal (SLIM) brain data repository, a publicly available database of neuroimaging and phenotypic data acquired from a large sample of Chinese young adults (fcon_1000.projects.nitrc.org/indi/retro/southwestuni_qiu_index.html) (7). The current sample included a large subset of participants who completed a battery of divergent thinking assessments, including the AUT (n = 405; 215 females, mean age = 20.03 y, age range = 1.25). All participants were right-handed with normal or corrected-to-normal vision and reported no history of neurological disorder, cognitive disability, or medication that affects the central nervous system. Participants completed consent forms and were paid for their time. The study was approved by the Southwest University Brain Imaging Center Institutional Review Board.

Behavioral assessment. The verbal form of the Torrance Tests of Creative Thinking (TTCT) (8) was used to assess creativity (i.e., divergent thinking ability). Five tasks from the Chinese version of the TTCT were administered: generating questions; causes and consequences; improving products; alternate uses; and manipulating objects. The TTCT provides a total creativity score as well as indices and scores for evaluating different creative processes or dimensions, which includes (*i*) fluency (the number of meaningful and relevant responses), (*ii*) flexibility (the number of different categories of responses), and (*iii*) originality (the degree of originality of the responses). Three trained raters coded the creative quality of responses consistent with conventional scoring procedures described in the TTCT manual (ICC > 0.90). Latent variable analysis was applied to extract a latent variable creativity score for each participant. We specified the latent variable using Mplus 7.2, indicated by the average fluency, flexibility, and originality scores. To assess fluid intelligence, participants completed the Combined Raven's Test (CRT) (72 items), a widely used intelligence assessment in China that is based on Raven's Color Progressive Matrices.

MRI data acquisition and preprocessing. Resting-state fMRI data were acquired for 8 min. Whole-brain imaging was performed on a 3T Siemens Trio MRI system (Siemens Medical Systems) using a 12-channel head coil. BOLD-sensitive T2*-weighted functional images were acquired using a single shot gradient-echo EPI pulse sequence (TR = 2,000 ms, TE = 30 ms, flip angle = 90°, 32 axial slices, 3.4 × 3.4 × 4.0 mm, FoV = 220 × 220 mm, interleaved slice ordering, 242 volumes) and corrected online for head motion. During functional imaging, participants were asked to keep their eyes closed, remain awake, and not think about anything in particular. A high resolution T1 scan was also acquired for anatomic normalization. Imaging data were preprocessed using SPM 12. The first 10 volumes from each subject's functional imaging data were discarded to account for steady-state magnetization, resulting in 232 volumes for subsequent analysis. Functional volumes were slice time-corrected, realigned, resliced to a voxel size of 3 mm^3, normalized to the MNI template brain, and smoothed with a 6-mm^3 isotropic Gaussian kernel. Additional preprocessing included regression of motion parameters, along with white matter and cerebrospinal fluid (CSF); BOLD time series were filtered using a standard low-pass filter (0.01–0.08 HZ).

1. Córdova NI, Tompary A, Turk-Browne NB (2016) Attentional modulation of background connectivity between ventral visual cortex and the medial temporal lobe. *Neurobiol Learn Mem* 134:115–122.
2. Benedek M, et al. (2014) To create or to recall? Neural mechanisms underlying the generation of creative new ideas. *Neuroimage* 88:125–133.
3. Shen X, Tokoglu F, Papademetris X, Constable RT (2013) Groupwise whole-brain parcellation from resting-state fMRI data for network node identification. *Neuroimage* 82:403–415.
4. Whitfield-Gabrieli S, Nieto-Castanon A (2012) Conn: A functional connectivity toolbox for correlated and anticorrelated brain networks. *Brain Connect* 2:125–141.
5. Fink A, et al. (2015) Training of verbal creativity modulates brain activity in regions associated with language- and memory-related demands. *Hum Brain Mapp* 36: 4104–4115.
6. Wallach MA, Kogan N (1965) *Modes of Thinking in Young Children* (Holt Rinehart and Winston Inc., New York).
7. Liu W, et al. (2017) Longitudinal test-retest neuroimaging data from healthy young adults in southwest China. *Scientific Data* 4:170017.
8. Torrance EP (1966) *Torrance Test of Creative Thinking* (Scholastic Testing Service, Inc., Bensenville, IL).

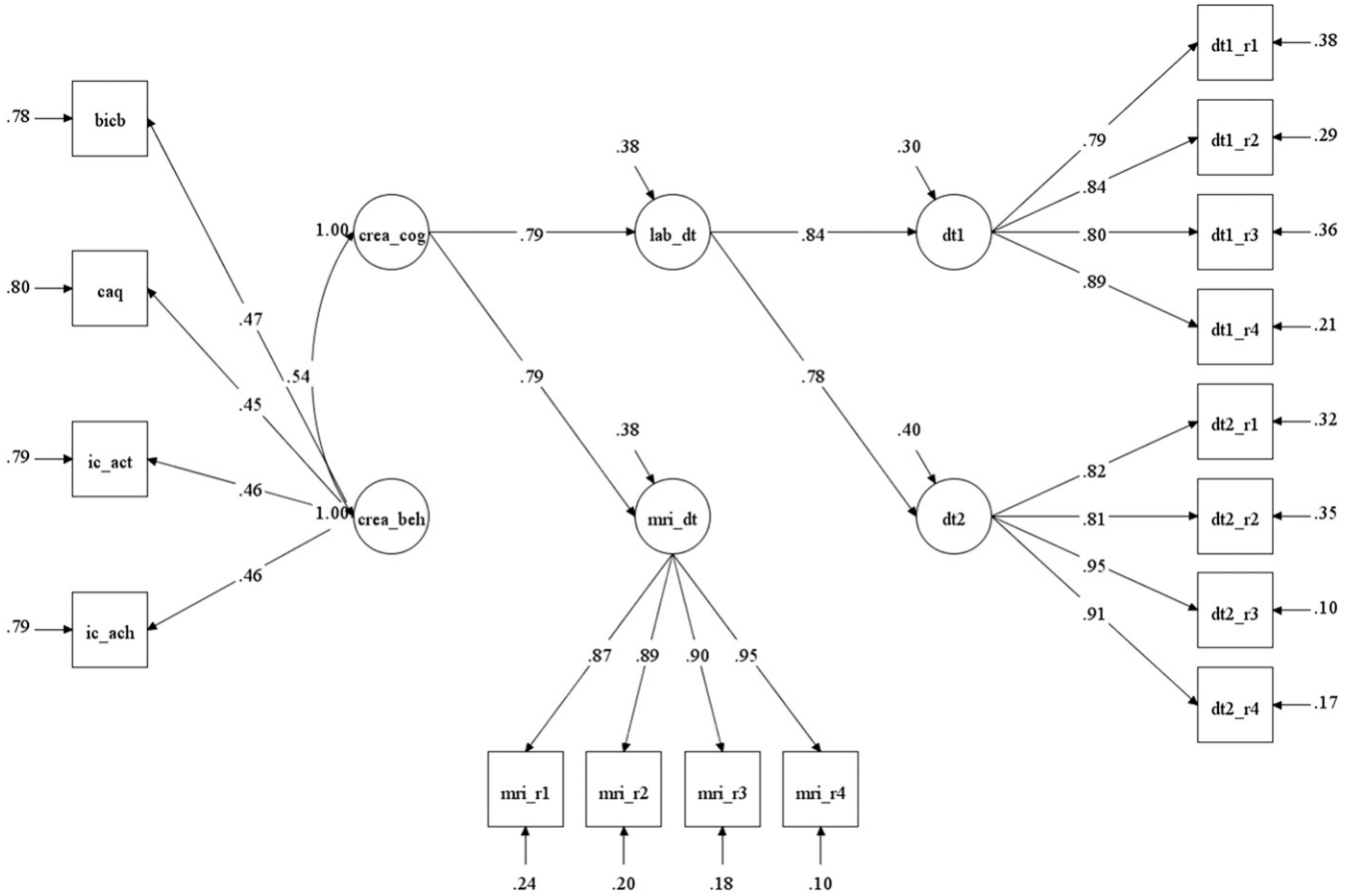

Fig. S1. Latent variable model of creative thinking and behavior. bicb, Biographical Inventory of Creative Behavior; caq, Creative Achievement Questionnaire; crea_beh, creative behavior; crea_cog, creative cognition (divergent thinking creativity); dt1, divergent thinking task 1 (laboratory responses); dt1_r1-r4, divergent thinking task 1 rater 1–4 scores (laboratory responses); dt2, divergent thinking task 2 (laboratory responses); ic_act = Inventory of Creative Activities; ica_ach = Inventory of Creative Accomplishments; mri_r1-r4 = divergent thinking 1–4 scores (in-scanner responses).

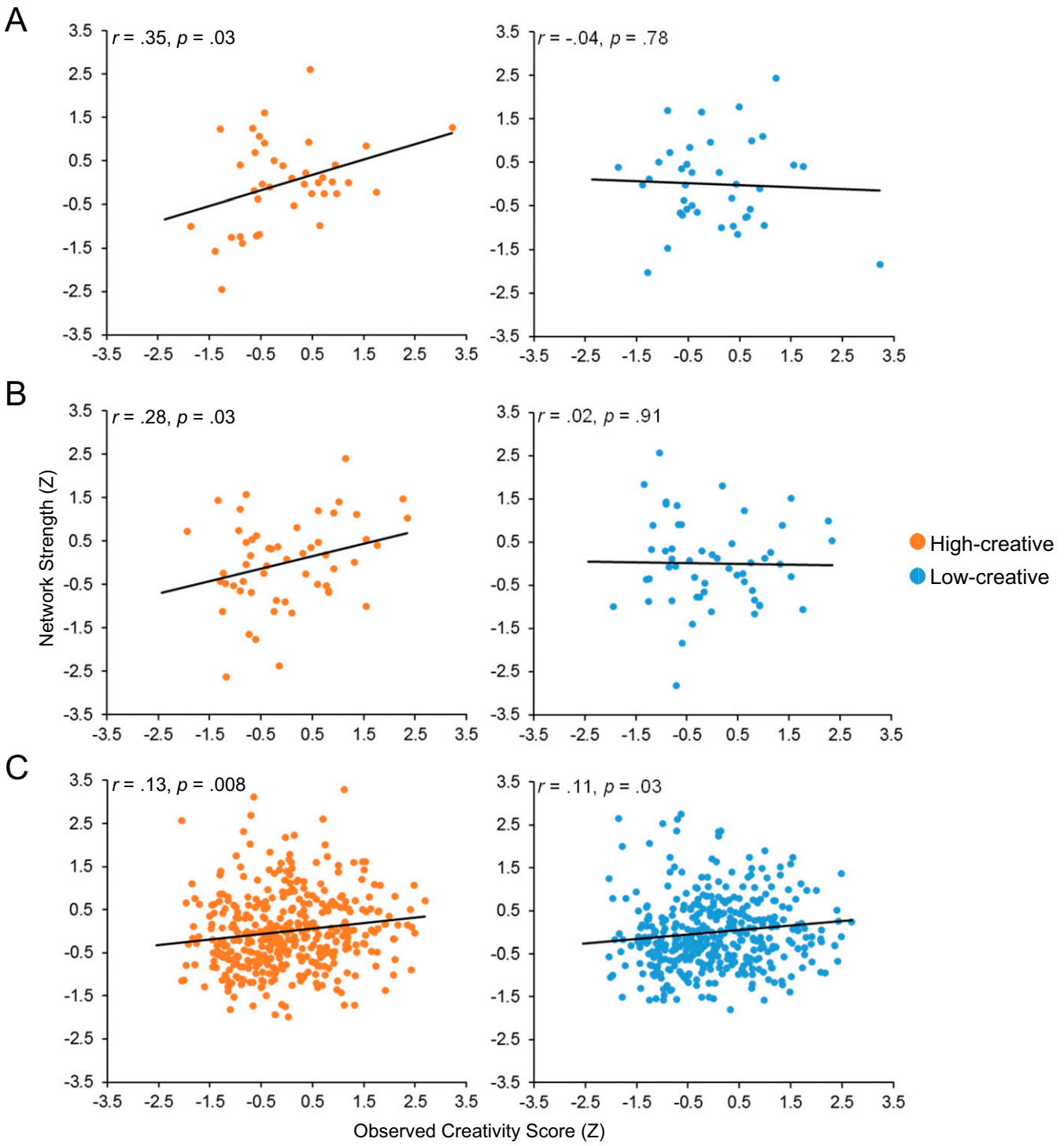

Fig. S2. Scatterplots for all external validation analyses. High- and low-creative network strength values and observed creativity scores are standardized for visualization. Correlations between high- and low-creative network strength in external validation 1 (*A*; task fMRI), external validation 2 (*B*; task fMRI), and external validation 3 (*C*; resting-state fMRI).

Table S1. High-creative network neuroanatomy (top 25 high-degree nodes)

No.	*K*	Node name	Network	L/R	Lobe	BA	MNI
1	19	Posterior cingulate	Default	L	Limbic	23	−5, −36, 32
2	15	Anterior insula	Cingular-opercular	L	Insula	13	38.7, 8.1, −4.8
3	14	Anterior insula	Salience	L	Prefrontal	45	−32.5, 22.1, 5.8
4	12	Precuneus	Default	L	Limbic	31	−6.5, −53.9, 37.4
5	9	Precuneus	Default	R	Limbic	31	6.2, −57.4, 38.2
6	8	Dorsolateral PFC	Frontal-parietal	R	Prefrontal	10	44.6, 46.2, −4.9
7	8	Anterior cingulate	Default	L	Limbic	32	−6, 34.1, 26.3
8	8	Posterior cingulate	Default	R	Subcortical	n/a	21.2, −36.4, 22.6
9	8	Anterior temporal	Default	R	Temporal	22	56.5, −8.5, −14.3
10	7	Precentral gyrus	Default	L	Prefrontal	8	−39.3, 1.7, 46.7
11	7	Dorsolateral PFC	Frontal-parietal	L	Prefrontal	9	46.1, 28.2, 26.8
12	7	Ventromedial PFC	Default	L	Prefrontal	11	−8.2, 39.7, −21.4
13	7	Midcingulate	n/a	R	Limbic	23	7, −18.8, 29.8
14	6	Caudate	n/a	L	Subcortical	n/a	−10.8, 23.9, 9.6
15	6	Retrosplenial	Default	L	Limbic	23	−8.6, −58.8, 17.6
16	6	Inferior frontal gyrus	Frontal-parietal	L	Prefrontal	44	−53.1, 18.4, 10.6
17	6	Calcarine	Visual	R	Limbic	23	28.4, −53.8, 7.1
18	6	Posterior cingulate	Default	R	Limbic	23	5.1, −38.9, 27
19	6	Ventromedial PFC	Default	R	Prefrontal	10	8.2, 45.9, −1.7
20	5	Crus 1	Cerebellum	L	Cerebellum	n/a	−40.3, −74.2, −29.1
21	5	Inferior frontal gyrus	n/a	L	Prefrontal	47	−32, 20.5, −16
22	5	Inferior frontal gyrus	n/a	L	Prefrontal	11	−18.2, 19, −21
23	5	Precuneus	Salience	R	Limbic	31	8.3, −39.9, 48.1
24	5	Precuneus	Default	R	Limbic	23	12.3, −57.2, 18.1
25	5	Anterior insula	Salience	R	Insula	13	37.5, 21.1, −10.1

BA, Brodmann area; K, degree; L, left; n/a, not available; PFC, prefrontal cortex; R, right.

Table S2. Low-creative network neuroanatomy (top 25 high-degree nodes)

No.	*K*	Region	Network	L/R	Lobe	BA	MNI
1	23	Brainstem	n/a	L	Brainstem	n/a	−7.2, −33, −39.4
2	23	Posterior cingulate	Default	L	Limbic	23	−5, −36, 32
3	21	Precuneus	Default	L	Limbic	31	−6.5, −53.9, 37.4
4	21	Brainstem	n/a	R	Brainstem	n/a	7.5, −34.2, −37.3
5	19	Fusiform gyrus	Visual	L	Occipital	19	−43.2, −70.4, −13.8
6	19	Brainstem	n/a	R	Brainstem	n/a	6, −22.2, −42.3
7	18	Primary motor cortex	Somato-motor	R	Parietal	40	52.8, −27.2, 40.9
8	18	Premotor cortex	Somato-motor	R	Parietal	1	32.4, −39.2, 49.6
9	17	Anterior insula	Cingular-opercular	L	Insula	13	−38.7, 8.1, −4.8
10	16	Anterior insula	Salience	L	Insula	45	−32.5, 22.1, 5.8
11	16	Inferior frontal gyrus	n/a	L	Prefrontal	11	−18.2, 12, −21
12	16	Cerebellum	n/a	R	Cerebellum	n/a	6.1, −50.7, −12.3
13	15	Cerebellum	n/a	L	Cerebellum	n/a	−6.5, −50.2, −11.4
14	14	Thalamus	Subcortical	L	Subcortical	n/a	−4.9, −10.3, 5.8
15	14	Thalamus	Subcortical	L	Subcortical	n/a	−9.6, −25.4, −1.4
16	14	Cerebellum	n/a	L	Cerebellum	n/a	−10.3, −37.7, −25.1
17	14	Hippocampus	Default	L	Limbic	n/a	−32.1, −40.2, −4
18	14	Retrosplenial cortex	Default	L	Limbic	23	−8.6, −58.8, 17.6
19	14	Thalamus	Subcortical	R	Subcortical	n/a	−10.5, −26.8, −2.2
20	14	Inferior frontal gyrus	n/a	R	Prefrontal	11	15.6, 34.1, −22.6
21	13	Brainstem	Subcortical	R	Brainstem	n/a	−5, −21.5, −15.8
22	13	Cerebellum	n/a	L	Cerebellum	n/a	−21.2, −53.4, −23.6
23	13	Midcingulate	Default	L	Limbic	31	−8.8, −42.6, 50.1
24	13	Fusiform gyrus	Visual	L	Occipital	19	−25.9, −63.1, −12.3
25	13	Brainstem	n/a	R	Brainstem	n/a	6.3, −24.9, −17.5

BA, Brodmann area; K, degree; L, left; n/a, not available; R, right.

Other Supporting Information Files

Dataset S1 (TXT)
Dataset S2 (TXT)